

# EVALUATION OF MAGNETIC ALLOYS FOR JHF RF CAVITY

Yoshio Tanabe\*<sup>1</sup>, Miho Fujieda\*<sup>2</sup>, Yoshiharu Mori, Hitoshi Nakayama, Chihiro Ohmori, Kazuyoshi Saito\*<sup>3</sup>, Yasuo Sato\*<sup>4</sup>, Tomonori Uesugi\*<sup>5</sup>, Masanobu Yamamoto\*<sup>6</sup> and Taixuan Yan\*<sup>7</sup>, KEK-Tanashi, 3-2-1 Midori-cho, Tanashi, Tokyo, 188, Japan  
Eiji Ezura, Akira Takagi and Masahito Yoshi, KEK, 1-1 Oho, Tsukuba-shi, Ibaraki-ken, 305, Japan

## Abstract

A new type of rf accelerating cavity using a high permeability magnetic alloy (MA) has been developed for the high intensity JHF proton synchrotrons. Compared with ordinary ferrites, the MA cores are very stable at high rf magnetic field and thus very high accelerating gradient (=accelerating voltage per cavity length) is available. We have measured several magnetic alloys in order to find a proper material for the cavity. In this paper, the test results are summarized and the evaluation of these materials is presented.

## 1 INTRODUCTION

In general, magnetic alloys have high permeability and low quality factor (Q value). An rf cavity loaded with the MA cores for high intensity proton synchrotron has many advantages [1]. Because the MA cores are stable up to the high rf magnetic field and have high Curie temperature, they can be used in high gradient operation [2]. Another advantage is to suppress the coupled bunch instability due to its low Q value [3]. If the Q value decreases from 30 to 1, the growth rate reduces by factor of 10. Furthermore, the MA core can make the cavity impedance broad. The MA loaded broad-band cavity does not need biasing circuit which sometimes causes the parasitic resonance.

Two materials were selected as the candidate of the cavity core. One is called FINEMET which is a Fe-based soft magnetic alloy composed of amorphous and ultra-fine grain [4,5]. Another one is an amorphous soft magnetic alloy.

We have measured the rf characteristics of these cores to find a suitable material for the JHF. This paper presents the results of the measurements and evaluation.

## 2 MEASURING METHOD

### 2.1 Fundamental Relations

The parallel complex permeability (suffix p) defined in equation (2) is adopted instead of the series expression (suffix s) in equation (1).

$$\mu = \mu_s' - j\mu_s'' \quad (1)$$

\*1 : also Toshiba Corporation \*2 : also NSRF, Kyoto Univ.  
\*3 : also Hitachi Corporation \*4 : also The Japan Steel Works Ltd.  
\*5 : also CNS, Univ. of Tokyo \*6 : also RCNP, Osaka Univ.  
\*7 : visiting scientist from the bureau of Basic Science of Academic China

$$1/\mu = 1/\mu_p' - 1/j\mu_p'' \quad (2)$$

Using the parallel expression, the inductance ( $L_p$ ) and the shunt resistance ( $R_p$ ) are expressed as; [6]

$$L_p = \mu_0/2\pi \times t \times \mu_p' \times \ln(b/a) \quad (3)$$

$$R_p = \mu_0/2\pi \times \omega \times t \times \mu_p'' \times \ln(b/a) = \mu_0 \times t \times \ln(b/a) \times (\mu_p' Q_f) \quad (4)$$

$$Q = R_p/\omega L_p = \mu_p''/\mu_p' \quad (5)$$

where, a is an inner diameter, b is an outer diameter and t is a thickness of the core, respectively. The quality Factor (Q) is the same in both expressions.

The relation between  $\mu_s'$  and  $\mu_p'$  is shown in equation (6).

$$\mu_p' = \mu_s'(1 + 1/Q^2) \quad (6)$$

It should be noted from equation (6) that in the case of high Q,  $\mu_s'$  is nearly equal to  $\mu_p'$  but in the case of low Q, both expressions are different. Therefore, we should give attention for evaluating the MA cores using the parallel complex permeability.

### 2.2 Test Bench

A test bench to measure  $L_p$ ,  $R_p$  and Q of MA cores and ferrites, is shown in Figure 1 [7]. The test bench is a coaxial cavity composed of an inductance (MA) and a capacitance (vacuum capacitors). It can accept from large-sized core (diameter of 700mm) to small sample core (inner diameter of 30mm). The maximum rf power of 1kW is supplied from the rf feeder and the maximum bias current of 1000A is fed from the bias current feeders.

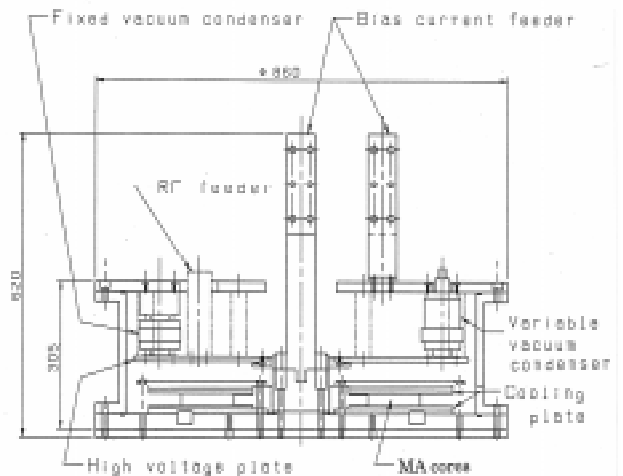


Figure 1. Cross section of the test bench for MA cores

### 3 MEASUREMENT RESULTS

Several FINEMETs and amorphous magnetic alloys listed in Table 1 have been tested.

Table 1. Test Samples of Magnetic Alloys (MA)

Material	Name	Comments
FINEMET	FT3M	Heat process without magnetic field, 18 $\mu$ m*
	FT3L	Heat process with axial magnetic field, 18 $\mu$ m*
	FT3H	Heat process with azimuthal magnetic field, 18 $\mu$ m*
	FT1H	Extremely low magnetostriction but low $\mu_p'Q_f$ .
	FT1L	Extremely low magnetostriction but low $\mu_p'Q_f$ .
Amorphous soft magnetic alloys	METGLAS	Fe-based, 23 $\mu$ m*.
	Fe-Ni	Fe-Ni based, 16 $\mu$ m*.
	Co	Co-based, low $\mu_p'Q_f$ .

\*: tape thickness

These cores have an inner diameter of 32mm, an outer diameter of 70mm and a thickness of 25mm. Promising four cores, FT3M, FT3L, METGLAS and Fe-Ni based core, are reported in this paper.

#### 3.1 Dependence of $\mu_p'Q_f$ on RF Magnetic Flux Density

The  $\mu_p'Q_f$  dependence on rf magnetic flux density (Brf) at 2MHz is shown in Figure 2. The Brf is obtained from,

$$B_{rf} = V_{rf} / \omega S \quad (7)$$

where  $V_{rf}$  and  $S$  mean the induced rf voltage and the cross sectional area of a core, respectively.

It is clear from Figure 2 that the  $\mu_p'Q_f$  of ferrites (Ni-Zn) is higher than that of FT3M and amorphous cores

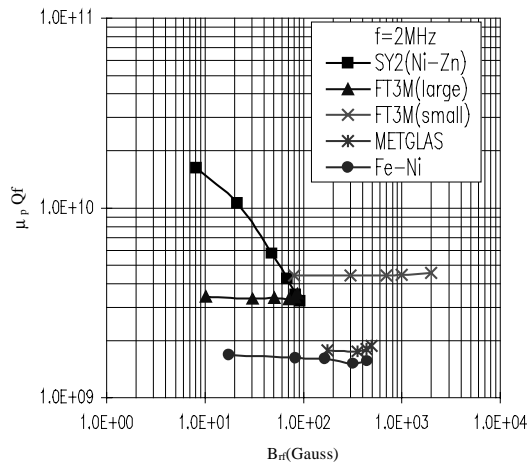


Figure 2.  $\mu_p'Q_f$  vs. Brf for MA cores and ferrite

under low Brf, but the  $\mu_p'Q_f$  of FT3M becomes higher over 100Gauss because it remains flat up to 2000Gauss.

The  $\mu_p'Q_f$  of the amorphous cores is about 1/3 of that of FT3M and nearly flat up to 500Gauss. Because in this case, the maximum Brf is limited by the capacity of rf power source, there is a possibility that the amorphous cores can be used over 500Gauss.

#### 3.2 RF Characteristics of Magnetic Alloys

As shown in Figure 3, the  $\mu_p'$  becomes low gradually as the frequency increases. The  $\mu_p'$  of FINEMET (FT3M and FT3L) is several 1000 around 2MHz and about 10 times higher than that of amorphous cores (METGLAS and Fe-Ni based core).

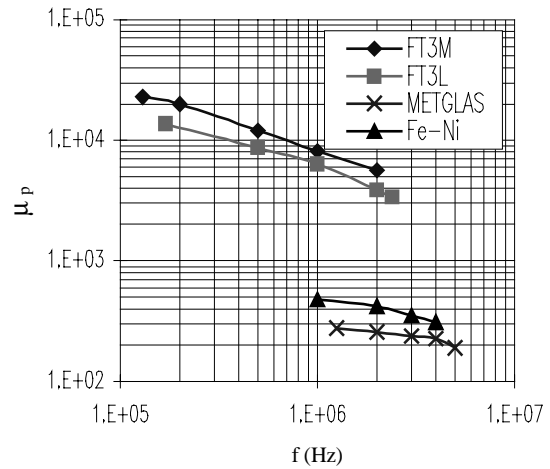


Figure 3. Comparison of parallel permeability ( $\mu_p'$ ) for four MA cores (2MHz)

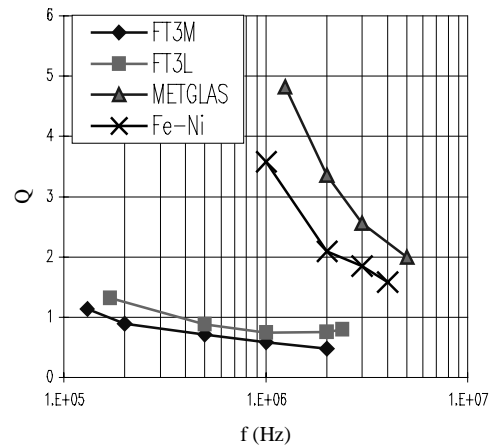


Figure 4. Comparison of Quality factor (Q) for four MA cores (2MHz)

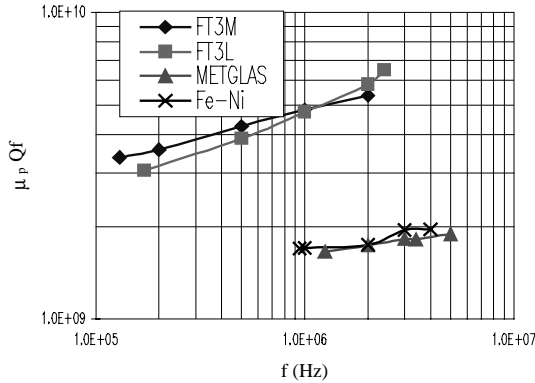


Figure 5. Comparison of  $\mu_p'Qf$  for four MA cores (2MHz)

The comparison of quality factor (Q) is presented in Figure 4. The Q values of FINEMET are below 1 and those of amorphous cores are from 2 to 3 around 2MHz.

Figure 5 shows the comparison of  $\mu_p'Qf$ . Both  $\mu_p'$  and Q value become low at higher frequency as known from Figure 3 and Figure 4, but the product,  $\mu_p'Qf$ , becomes high as the frequency increases. The  $\mu_p'Qf$  of both FINEMET cores is about 3 times high compared with the amorphous cores because of their high permeability ( $\mu_p'$ ).

### 3.3 Dependence of permeability and Q on Bias Field

Figure 6 shows the dependence of the  $\mu_p'$  on the DC bias magnetic field at 2MHz. FINEMETs are very sensitive to the bias field and therefore we can easily change the resonant frequency of rf cavity, if necessary. On the other hand, the amorphous cores are not sensitive to the bias field. For example, the  $\mu_p'$  of METGLAS hardly changes by the bias field.

Figure 7 shows the dependence of the Q value on the DC bias magnetic field at 2MHz. The Q values become large as the bias field increases and the  $\mu_p'Qf$  of the amorphous cores increases because the change of their  $\mu_p'$  is small as seen from Figure 6.

## 4 CONCLUSION

The rf characteristics of the MA cores have been measured and evaluated. Several MA cores are stable even under high rf magnetic flux density and therefore they can be used in high gradient operation. Because FINEMET cores have high  $\mu_p'Qf$ , the JHF rf cavities become compact by adopting them. On the other hand, the amorphous cores have high Q value and they will become promising candidate, if higher Q value is required.

Above-mentioned results have been acquired from small samples except FT3M. It is necessary for future study to measure the core of actual size.

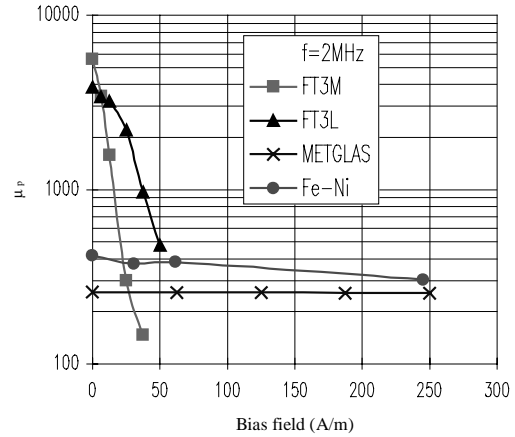


Figure 6. DC bias field dependence of  $\mu_p'$

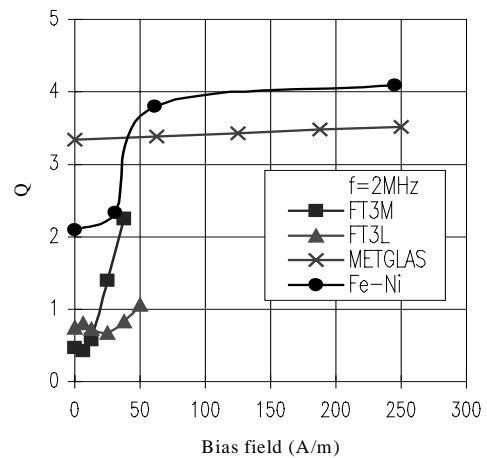


Figure 7. DC bias field dependence of Q

## REFERENCES

- [1] C. Ohmori et al., Proceedings of 1997 Particle Accelerator Conference, Vancouver, Canada, 1997.
- [2] Y. Mori et al., Proceedings of 11th Symposium on Accelerator Science and Technology (1997) 224.
- [3] T. Uesugi et al., Proceedings of 1997 Particle Accelerator Conference, Vancouver, Canada, 1997.
- [4] M. Fujieda et al., Proceedings of 1997 Particle Accelerator Conference, Vancouver, Canada, 1997.
- [5] T. Uesugi et al., Proceedings of 11th Symposium on Accelerator Science and Technology (1997) 188.
- [6] I. S. K. Gardner, CERN Accelerator School, CERN-92-03 (1992) 352.
- [7] Y. Tanabe et al., Trans. IEE of Japan, Vol.117-A, No.9, Sep., 1997, 930 (in Japanese)